IEEE Access
Multidisciplinary ⋮ Rapid Review ⋮ Open Access Journal

Received 29 April 2026, accepted 11 May 2026, date of publication 20 May 2026, date of current version 19 June 2026.
Digital Object Identifier 10.1109/ACCESS.2026.3695045

RESEARCH ARTICLE

Performance Enhancement of Cooperative NOMA in Satellite Communication Through Combining Techniques

K. ASHWINI[1], ASHISH SINGH[2], (Member, IEEE), JAGADEESH V. K.[3], (Senior Member, IEEE), RACHANA SHENOY[1], AND DUSHANTHA NALIN K. JAYAKODY[4,5], (Senior Member, IEEE)
[1]Department of Electronics and Communication Engineering, NMAM Institute of Technology (NMAMIT), NITTE (Deemed to be University), Nitte 574110, India
[2]Department of Computer and Communication Engineering, NMAM Institute of Technology (NMAMIT), NITTE (Deemed to be University), Nitte 574110, India
[3]Department of Electronics and Communication Engineering, National Institute of Technology Calicut, Kozhikode 673601, India
[4]INESC INOV Lab, ECATI, Universidade Lusófona, 1749-024 Lisbon, Portugal
[5]CIET, Faculty of Engineering, Sri Lanka Institute of Information Technology, Malabe 10115, Sri Lanka

Corresponding author: K. Ashwini (ashwinik@nitte.edu.in)

ABSTRACT This article studies the analysis of the key performance parameters in the proposed cooperative Non-Orthogonal Multiple Access (NOMA) system considering the satellite network. NOMA can be coupled with standard relaying procedures to increase the overall capabilities of the wireless communication system. The system under consideration consists of two users, one near and a far user, and a satellite. The paper explores by using a Decode and Forward (DF) relaying mechanism at the user closer to the satellite, which will forward the signal received from the satellite user that is distant from it. In separate case studies, the far user combines the direct and indirect transmission signals using Maximal Ratio Combining (MRC) and Selection Combining (SC) techniques. The expressions for outage, average Bit Error Rate (BER), and capacity are derived for MRC and SC methods. It is also derived and approximated, and closed-form expressions are obtained. The simulation results of these analytical expressions reveal that the MRC method of combining outperforms the SC technique in terms of outage, BER, and ergodic capacity.

INDEX TERMS Cooperative relaying, decode and forward, NOMA, relaying techniques, diversity combining.

I. INTRODUCTION

Multiple access strategies have expanded dramatically in recent years to meet the demands of the network in high-density locations [1]. As wireless information communication advanced to the fifth generation (5G) from the first generation (1G), more applications emerged with high data rate requirements, lower delays and enhanced spectral efficiency. It is unlikely to satisfy these needs since Orthogonal Multiple Access (OMA) is used in mobile communication to divide resources among different users and applications. Hence, there is a need for new developments in multiplexing techniques [2], [3]. A viable multiple access method that could meet each of these requirements has been demonstrated to be Non-Orthogonal Multiple Access (NOMA) [4], [5].

The core notion associated with NOMA is to distribute power among mobile users based on their channel conditions [6]. The traditional concept of OMA had low spectral efficiency when considering the channel conditions of weak users far from the satellite station [7]. This drawback is overcome in NOMA technology, where the spectral efficiency is improved [8]. NOMA is separated into two groups: code-domain NOMA and power-domain NOMA. In power domain NOMA, the transmitter generates a superposition-coded symbol for the users. Each user is simultaneously given a different power level on the same frequency based on the quality of the channel. The weak mobile user has power allocated more than the strong mobile user nearer to the transmitter. On the other hand, code-domain NOMA is comparable to multi-carrier code division

The associate editor coordinating the review of this manuscript and approving it for publication was Arun Prakash.

multiple access (CDMA) [9]. NOMA allows several users or the base station (BS) to transmit signals in a superposition fashion, in contrast to traditional OMA [10] methods like CDMA, Time Division Multiple Access (TDMA), Frequency Division Multiple Access (FDMA), etc. By sharing the time, coding, and frequency resources of the channel, NOMA can allow multiple users to transmit data simultaneously. Nevertheless, the signals have different strengths [10], [11]. Additionally, NOMA offers a number of benefits, including more connectivity, effective spectrum use, and multiple user support. The NOMA shares a single frequency channel [12], as opposed to sharing the available bandwidth across several users.

Due of the variations in signal strengths in NOMA, the receiver can use the Successive Interference Cancellation (SIC) technique to interpret the information signal intended for each user [13], [14].

NOMA systems may be applied together with the cooperative relaying approach to improve performance further. The two types of Cooperative NOMA (CNOMA) are relay-assisted and user-assisted. When adopting user-assisted CNOMA, improved channel conditions enable users to work like a relay to help weaker users perform better [15], [16]. There are two methods for relaying signals: Amplify and forward (AF) and Decode and forward (DF). AF uses an amplification factor to increase the strength of the signal it receives. DF decodes the received signals and only sends the decoded signal to the next user. A DF relay is substantially more sophisticated than an AF relay, as it has full processing capacity. In general, a DF relay is almost as sophisticated as a BS [17], [18]. In AF since the signal is amplified and sent, the noise component is also amplified, which can degrade its performance. This would also result in more power consumption. As described in [19], a CNOMA signal transmission approach exploits the fact that certain users in systems using NOMA have knowledge of the messages sent by others beforehand. In typical Cooperative relay systems (CRS), the receiver can acquire one bit of information, whereas the proposed receiver in [19] is capable of receiving two data symbols in two slots of time reliably. This approach with CNOMA outperforms previous cooperative relaying approaches for greater channel powers across a wide range of the transmit SNR regime. To increase the NOMA performance gain, this work analyzes a cooperative DF relay configuration that uses NOMA across Rician fading channels. Results showed that CNOMA beats standard NOMA in terms of achievable rate.

The most popular method of improving wireless communication networks and their dependability is through diversity techniques [20]. It has long been known that the use of multiple copies of the incoming communication signal can effectively reduce fading and associated negative effects on the performance of the communication system [21]. To improve the signal-to-noise ratio (SNR) on the receiver side, the fundamental purpose of diversity is to recover information from the signal that was delivered through several fading channels [22]. Many types of diversity receiver operate across a range of fading channels. Maximal ratio combining (MRC), Selection combining (SC), and Equal gain combining (EGC) are three frequently used diversity strategies.

As a diversity scheme in a communication system, MRC symbolizes an ideal combiner over fading channels in theory. In this technique, the instantaneous SNR at the output will be maximized by combining several copies of the same information signal. In SC, the highest SNR is chosen among all received branches. It is assumed that the receiver has the necessary knowledge about channel fading in every scenario. In contrast, the signals received in EGC are added after being similarly weighted [23].

NOMA can also be employed in satellite communication to enhance overall performance. In [24] some of the techniques and architectures in NOMA based satellite communication were discussed and their future scope was also provided. In [25] the performance of a CRS NOMA comprising a BS and two users that use Rician fading channels was assessed. The simulation findings demonstrate that the suggested Dynamic compressed sensing with Multiuser Detection (DCS-MUD) and CRS NOMA across behave significantly well compared to the classic CS-MUD and traditional CRS. The performance of the NOMA-based CRS was studied by obtaining exact mathematical formulations to determine the achievable rates under the Rician fading channel [26]. An effective approximation approach called Gauss-Chebyshev Integration was applied for achievable rate derivation. The results revealed that the NOMA-based CRS can achieve a better achievable rate than the conventional CRS. In [27], a DF Full Duplex (FD) relaying system with an eavesdropper were investigated. Using SC and MRC techniques at the receivers' side the precise equations for intercept probability (IP) and outage probability (OP) were determined. According to the simulations, the MRC method's OP and IP outperformed the SC method's. The performance of a satellite source that has a receiver on the ground is investigated, along with another source that uses CRS NOMA to transmit the signal to two users. It significantly improved performance when CRS NOMA is used with the cognitive hybrid satellite terrestrial network underlay [28]. From reviews in the literature, a user-aided cooperative NOMA strategy implementing combining techniques has yet to be explored in the field of satellite communication. Its performance could provide an avenue for further exploration of research. Although NOMA has an advantage in terms of spectral efficiency to a significant extent. Its practical implementation is greatly affected by the hardware impairments of the Radio Frequency (RF) chains at the BS and at users [29], [30], [31].

In this paper, the study of the performance of NOMA-based CRS, having one near user and a far user, a satellite is carried out. As a CRS strategy, DF relay is used.

The main contributions of the work are to analyze and compare performance indicators like OP, average Bit Error Rate (BER), and ergodic capacity employing MRC and SC combined techniques at the destination mobile user. In the system, the nearest user works as a relay to forward the signal to the distant mobile user. As a result, two separate signals are acquired at the location where these combining methods can be applied. The analytical expression for OP, BER, and ergodic capacity is obtained for data signals from both users and is simulated. The paper is structured in the following manner: Section II outlines the system model proposed. Section III shows the mathematical calculations for developing the expressions for OP, BER, and ergodic capacity. Section IV discusses the results of the analytical calculations. Section V provides the conclusion of the work.

A. MOTIVATION AND CONTRIBUTIONS

Better user fairness and increased spectrum utilisation are possible with the CNOMA technique. Since satellite communication needs to serve many users with variable channel conditions, this technique provides better coverage because strong users can function as a relay to send the signal to weak users. Rician fading represents one strong line-of-sight (LOS) situation which is the environmental condition for indoor application and in satellite communication as well. Rician channel also exhibits multipath effects which represent a satellite communication environment effectively. From the literature survey, the evaluation of MRC and SC techniques in a CNOMA over a Rician fading channel is yet to be explored and studied. This became the main motive for the analysis. The key contributions are

- Using the probability density function (PDF) and cumulative density function (CDF), an exclusive equation that represents the OP at the destination, BER, and ergodic capacity through Rician channels is constructed for the proposed system.
- The proposed system employs a DF relaying for the cooperative technique. The diversity combining schemes, like MRC and SC, are applied at the destination for combining different branch signals.

B. SCOPE, MULTI-USER EXTENSIONS, AND FAIRNESS VIA DYNAMIC POWER CONTROL

Although our closed-form outage analysis concentrates on a two-user configuration, it can also be extended to a multi-user environment, which is common in satellite communication systems. In a multi-user scenario, each k-th user, before detecting its own signal ($1 < k < U$), must first decode the message signal meant for users with worse channel conditions. Specifically, the k-th user decodes the messages $M_{1,j}$ for $U \geq j \geq (k+1)$ [32].

The signal-to-interference-plus-noise ratio (SINR) for this decoding process at user j while decoding user k's signal is given by

$$\mathrm{SINR}_{1,j} = \gamma_{j\to k} = \frac{p_k G_j}{\sum_{l=k+1}^{U} p_l G_j + N_0} \tag{1}$$

where G_j denotes the combined channel gain under (SC) or MRC. The message $M_{1,j}$ is decoded successfully if

$$\mathrm{SINR}_{1,j} \geq \gamma_{\mathrm{kth}}, \tag{2}$$

where γ_{kth} is the threshold SINR required to decode the k-th user's signal for all $j \geq k$. This relationship generalizes the two-user SIC condition employed in our analysis [33].

The effective SINR expressions depend on the combined channel gain, which differs for MRC and SC techniques.

MAXIMAL RATIO COMBINING (MRC)

Under MRC, the combined channel gain at user j is expressed as

$$G_j = \sum_{b=1}^{B} |h_{j,b}|^2. \tag{3}$$

This approach yields the highest average SNR and the largest diversity gain.

SELECTION COMBINING (SC)

Under SC, the combined channel gain is given by

$$G_j = \max_{b} |h_{j,b}|^2. \tag{4}$$

This results in a lower combined gain compared to MRC.

Consequently, MRC makes it easier to satisfy the SIC condition in (1) compared to the SC technique.

The two optimization problems considered in this scenario—Max–Min Rate Fairness (P-Fair) and Outage-Constrained Power Optimization (P-OP)—are strongly dependent on the outage probability. Therefore, the solutions to (P-Fair) [34] and (P-OP) [35] are governed by how MRC and SC affect the distribution of G_j. Since MRC provides higher diversity, improved average SNR, and reduced outage probability, the feasible power allocation region for achieving multi-user fairness targets is naturally expanded.

II. SYSTEM MODEL

Figure 1. depicts the system model, which comprises two users, one far away marked by U2, and one close to the satellite marked by U1. All channels are considered Rician channels, and all channels experience an Additive White Gaussian Noise (AWGN) on the receiving terminal. The Rician fading channel assumes one strong LOS path. Rician fading is considered in mobile radio channels along with indoor Cordless Telecommunications (CT), although the rayleigh model is considered the most popular [36]. In rural areas of mobile communication, you typically have a channel with a dominant component of the LOS. In order to compare performances of two techniques of combining, a known parameter is able to analyse the performance in terms of OP and provide closed-form expressions for the key performance indicators. Hence, in the system analysis, the Rician fading

parameter (K factor) is assumed to be known. Let h_{b1}, h_{b2} and h_{12} indicate the coefficients of the channels from satellite to U1, U2 and from user U1 to U2 respectively. Also, let n_{b1}, n_{b2} and n_{12} signify the AWGN from satellite at U1, U2, and from user U1 to U2, respectively. It has mean zero and variance σ^2.

The CNOMA distribution is split into two time intervals. The satellite will employ the NOMA technique for delivering the signal to the user nodes during the first time phase. The superimposed signal that is delivered to user U1, which will direct the signal towards U2 in the second time phase. The DF relay protocol is implemented by U1. At the first phase of time, the superimposed signal that is delivered at U1 from the satellite is expressed as

$$y_{b1} = h_{b1}\left[x_1\sqrt{a_1P_{tx}} + x_2\sqrt{a_2P_{tx}}\right] + n_{b1} \tag{5}$$

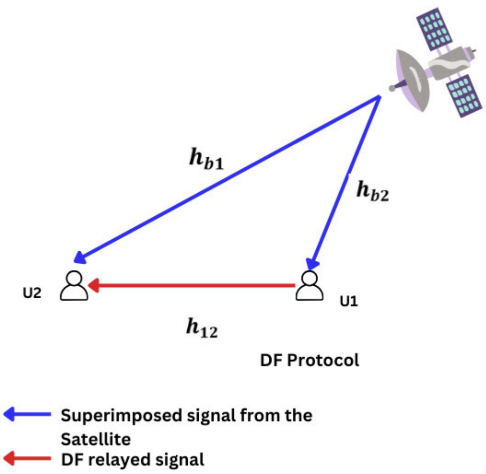

FIGURE 1. System model with DF-based CNOMA.

where the information signals meant for U1 and U2 are denoted by x_1 and x_2, respectively. The power allocation coefficients for users U1 and U2 are a_1 and a_2, respectively. They are carefully selected so that $a_1 + a_2 = 1$ and $a_2 > a_1$. Let P_{tx} be the power transmitted from the satellite. The user U1 decodes x_2 signal now treating the signal x_1 as interference. The SINR of signal x_2 at U1 is expressed as follows

$$\gamma_{1,2}^{[1]} = \frac{|h_{b1}|^2 a_2P_{tx}}{|h_{b1}|^2 a_1P_{tx} + \sigma^2} \tag{6}$$

Hence, after performing SIC, U1 decodes its own information. Hence the signal-to-noise ratio (SNR) at U1 for decoding signal x_1 can be expressed as

$$\gamma_{1,1}^{[1]} = \frac{|h_{b1}|^2 a_1P_{tx}}{\sigma^2} \tag{7}$$

$$\gamma_{1,1}^{[1]} = |h_{b1}|^2 a_1\rho \tag{8}$$

where the signal power to noise power ratio is given as $\rho = \frac{P_{tx}}{\sigma^2}$. The signal delivered at U2 in the first phase from the satellite is as follows

$$y_{b2} = h_{b2}\left[x_1\sqrt{a_1P_{tx}} + x_2\sqrt{a_2P_{tx}}\right] + n_{b2} \tag{9}$$

At U2 after receiving the signal from the satellite, the SINR of obtaining x_2 is given as

$$\gamma_{2,2}^{[1]} = \frac{|h_{b2}|^2 a_2P_{tx}}{|h_{b2}|^2 a_1P_{tx} + \sigma^2} \tag{10}$$

$$\gamma_{2,2}^{[1]} = \frac{|h_{b2}|^2 a_2\rho}{|h_{b2}|^2 a_1\rho + 1} \tag{11}$$

The acting relay U1 uses DF strategy to transmit signal x_2 decoded from SIC and redirect the signal towards U2 during the second phase of time. Next, the signal that was received at U2 can be expressed as

$$y_{12} = h_{12}\left\{x_2\sqrt{P_r}\right\} + n_{12} \tag{12}$$

where P_r is the transmitted power from U1. Let $P_r = P_{tx}$ for simplification purpose. After the signal is acquired at U2, the SNR of x_2 signal is given as

$$\gamma_{2,2}^{[2]} = \frac{|h_{12}|^2 P_{tx}}{\sigma^2} \tag{13}$$

Hence,

$$\gamma_{2,2}^{[2]} = |h_{12}|^2\rho \tag{14}$$

III. SYSTEM PERFORMANCE

A. CHANNEL OF STATISTICS

Path loss, shadowing, and fading all have an impact on the performance of radio channels in wireless communication systems [37], [38]. Rician fading exhibits one strong LOS signal with multiple scattered signals. The Rician fading channel PDF is represented as

$$f_X(r) = \frac{r}{\sigma_r^2} e^{-\left(\frac{r^2+V^2}{2\sigma_r^2}\right)} I_0\left(\frac{rV}{\sigma_r^2}\right) \tag{15}$$

The CDF is given by

$$F_X(r) = 1 - Q_1\left(\frac{V}{\sigma_r}, \frac{r}{\sigma_r}\right) \tag{16}$$

$$= 1 - Q_1\left(\sqrt{2K}, \sqrt{\frac{2(K+1)}{\Omega}}\,r\right) \tag{17}$$

where r is the independent and identically distributed Gaussian random variable (i.i.d.), each with variance σ_r^2 and zero mean [39]. V is the non-centrality parameter. $I_0(.)$ symbolizes the modified Bessel function of the first kind of order zero. There are two more parameters associated with Rician channel. These are the K-factor or Rice factor, where $K = \frac{V^2}{2\sigma_r^2}$, is the power ratio of the LOS component to the non-LOS component, and Ω is the average total power, where $\Omega = V^2 + 2\sigma_r^2$ [40]. The parameters $V^2 = \frac{K}{K+1}\Omega$, $2\sigma_r^2 = \frac{\Omega}{1+K}$. The Marcum function Q is expressed as

$$Q_v(a, b) = \frac{1}{a^{v-1}}\int_b^\infty x^v e^{\left(-\frac{x^2+a^2}{2}\right)} I_{v-1}(ax)dx \tag{18}$$

where $b \geq 0$, and $a, v > 0$. I_{v-1} denotes the modified Bessel function of first kind with its order $v - 1$.

B. OUTAGE PROBABILITY

The OP defines the probability that the SINR threshold for the user is not reached. Let γ_{th} be the threshold SINR. In the first phase, the OP obtained at U1 of signal x_2 is given as

$$Pr\left(\gamma_{1,2}^{[1]} < \gamma_{th}\right) = Pr\left(\frac{|h_{b1}|^2 a_2 P_{tx}}{|h_{b1}|^2 a_1 P_{tx} + \sigma^2} < \gamma_{th}\right) \tag{19}$$

$$Pr\left(|h_{b1}|^2 < \frac{\gamma_{th}}{(a_2 - a_1\gamma_{th})\,\rho}\right) \tag{20}$$

and the OP at U1 of signal x_1 that is near the satellite is given as

$$Pr\left(\gamma_{1,1}^{[1]} < \gamma_{th}\right) = Pr\left(|h_{b1}|^2 a_1 \rho < \gamma_{th}\right) \tag{21}$$

$$= Pr\left(|h_{b1}|^2 < \frac{\gamma_{th}}{a_1\rho}\right) \tag{22}$$

where $\gamma_{th} = 2^R - 1$, with R indicating the target rate. OP at U2 of signal x_2 during the first time phase is given by

$$Pr\left(\gamma_{2,2}^{[1]} < \gamma_{th}\right) = Pr\left(\frac{|h_{b2}|^2 a_2\rho}{|h_{b2}|^2 a_1\rho + 1} < \gamma_{th}\right) \tag{23}$$

$$Pr\left(|h_{b2}|^2 < \frac{\gamma_{th}}{(a_2 - a_1\gamma_{th})\,\rho}\right) \tag{24}$$

After DF relaying by U1 in the second time slot, the OP at U2 of signal x_2 is provided as

$$Pr\left(\gamma_{2,2}^{[2]} < \gamma_{th}\right) = Pr\left(|h_{12}|^2 \rho < \gamma_{th}\right) \tag{25}$$

$$= Pr\left(|h_{12}|^2 < \frac{\gamma_{th}}{\rho}\right) \tag{26}$$

Given that the receiver receives two copies of the signal at U2, the combined techniques at U2 aid in improving the received SNR. Two cases are considered in which MRC and SC techniques are implemented to receive the signal. The SNR of each branch is added and assessed in the MRC method. Using MRC, the total SNRs γ_t taking into account all SNRs from branches B is provided as

$$\gamma_t = \sum_{j=0}^{B} \gamma_j \tag{27}$$

where γ_j is the SNR of each branch and $j = 1, 2 \ldots B$. Hence, the resultant OP is expressed for the decoding signal x_2 as

$$R_{OP} = Pr(\gamma_{1,2}^{[1]} < \gamma_{th}) \cdot Pr(\gamma_{2,2}^{[1]} < \gamma_{th}) + Pr(\gamma_{1,2}^{[1]} \geq \gamma_{th}) \cdot OPMRC \text{ or } OPSC \tag{28}$$

where *OPMRC* indicates the probability of an outage when MRC is implemented and *OPSC* indicates the probability of an outage for the SC technique. From (20),

$$Pr(\gamma_{1,2}^{[1]} < \gamma_{th}) = 1 - Q_1\left(\sqrt{2K}, \sqrt{\frac{2(1+K)}{\Omega_{SR}}\frac{\gamma_{th}}{(a_2 - a_1\gamma_{th})\rho}}\right) \tag{29}$$

Let,

$$OPMRC = Pr\left(\left(\gamma_{2,2}^{[2]} + \gamma_{2,2}^{[1]}\right) < \gamma_{th}\right) \tag{30}$$

$$Pr\left((A + B) < \gamma_{th}\right) = \int_0^{\gamma_{th}} F_A\left(\gamma_{th} - y\right) f_B\left(y\right) dy \tag{31}$$

Let,

$$F_A\left(x\right) = \Pr(A < x) \tag{32}$$

comparing (30) with (31), and substituting in (32). Let $A = \gamma_{2,2}^{[2]}$ and $B = \gamma_{2,2}^{[1]}$.

$$F_A\left(x\right) = Pr\left(\gamma_{2,2}^{[2]} < x\right) \tag{33}$$

Hence using equation (26),

$$Pr\left(\gamma_{2,2}^{[2]} < x\right) = 1 - Q_1\left(\sqrt{2K}, \sqrt{\frac{2(1+K)}{\Omega_{RD}}\frac{x}{\rho}}\right) \tag{34}$$

Substituting (34) in $F_A(x)$ we get

$$F_A\left(x\right) = 1 - Q_1\left(\sqrt{2K}, \sqrt{\frac{2(1+K)}{\Omega_{RD}}\frac{x}{\rho}}\right) \tag{35}$$

Next, using (24) to find $f_B(y)$, we obtain

$$F_B\left(y\right) = Pr\left(|h_{b2}|^2 < \frac{y}{(a_2 - a_1 y)\,\rho}\right) \tag{36}$$

$$= 1 - Q_1\left(\sqrt{2K}, \sqrt{\frac{2(1+K)}{\Omega_{SD}}\frac{y}{(a_2 - a_1 y)\rho}}\right) \tag{37}$$

with $0 < y < 1$. The following expression can be used to get the PDF of variable B.

$$f_B\left(y\right) = \frac{\partial F_B\left(y\right)}{\partial y} \tag{38}$$

Substituting (37) in (38) the following series of expressions are generated by partial differentiation with respect to y. The modified Bessel function of first kind with order v can also be expressed from (8.445) in [41] as

$$I_v(z) = \left(\frac{1}{2}z\right)^v \sum_{k=0}^{\infty} \frac{\left(\frac{1}{4}z^2\right)^k}{k!\Gamma(v + k - 1)} \tag{39}$$

Using (18) and (39) for $v = 1$, we get

$$Q_1\left(a, b\right) = \sum_{k=0}^{\infty} \left(\frac{a}{2}\right)^{2k} \frac{1}{(k!)^2} e^{-\frac{a^2}{2}} \int_b^{\infty} x^{2k+1} e^{-\frac{x^2}{2}} dx \tag{40}$$

Let $a = \sqrt{2K}$ and $b = \sqrt{\frac{2(1+K)}{\Omega_{SD}}\frac{y}{(a_2 - a_1 y)\rho}}$. The expression for $f_B\left(y\right)$ is obtained using the expression of the incomplete gamma function [41] in (40) as follows. Let $u = \frac{x^2}{2}$, the (40) then becomes,

$$Q_1(a, b) = \sum_{k=0}^{\infty} \left(\frac{a^2}{2}\right)^k \frac{e^{-\frac{a^2}{2}}}{(k!)^2} \int_{\frac{b^2}{2}}^{\infty} u^{k+1-1} e^{-u} du \tag{41}$$

$$Q_1(a, b) = \sum_{k=0}^{\infty} \left(\frac{a^2}{2}\right)^k \frac{e^{-\frac{a^2}{2}}}{(k!)^2} \Gamma\left(k + 1, \frac{b^2}{2}\right) \tag{42}$$

Hence,

$$f_Y(y) = \frac{\partial(F_Y(y))}{\partial y} = \frac{\partial(1 - Q_1(a, b))}{\partial y} \tag{43}$$

Substituting (42) in (43), the equation becomes

$$f_Y(y) = \frac{\partial}{\partial y}\left(1 - \sum_{k=0}^{\infty}\left(\frac{a^2}{2}\right)^k \frac{e^{-\frac{a^2}{2}}}{(k!)^2}\Gamma\left(k+1, \frac{b^2}{2}\right)\right) \tag{44}$$

Taking partial differentiation, the expression can be simpliflies as shown below.

$$\frac{\partial}{\partial y}\left(\Gamma\left(k+1, x\right)\right) = \frac{\partial \Gamma(k+1,x)}{\partial x}\cdot\frac{\partial x}{\partial y}$$

where $x = \frac{b^2}{2}$, Substituting b we get

$$x = \frac{2(1+K)y^2}{\Omega_{SD}(a_2 - a_1 y)^2 2\rho^2} \tag{45}$$

, hence

$$\frac{\partial x}{\partial y} = \frac{2(1+K)a_2 y}{\Omega_{SD}\rho^2(a_2 - a_1 y)^3} \tag{46}$$

$$\frac{\partial \Gamma(k+1,x)}{\partial y} = -(x)^{k+1-1}\cdot e^{-x} \tag{47}$$

$$\frac{\partial}{\partial y}\left(\Gamma\left(k+1, x\right)\right) = -\left(\frac{(1+K)y^2}{\Omega_{SD}(a_2 - a_1 y)^2\rho^2}\right)^k \cdot e^{-\frac{(1+K)y^2}{\Omega_{SD}(a_2 - a_1 y)^2\rho^2}}\frac{2(1+K)a_2 y}{\Omega_{SD}\rho^2(a_2 - a_1 y)^3} \tag{48}$$

$$f_Y\left(y\right) = -\sum_{k=0}^{\infty}\left(\frac{a^2}{2}\right)^k \frac{e^{-\frac{a^2}{2}}}{(k!)^2}\left[-\left(\frac{(1+K)y^2}{\Omega_{SD}(a_2 - a_1 y)^2\rho^2}\right)^k\right] \cdot e^{-\frac{(1+K)y^2}{\Omega_{SD}(a_2 - a_1 y)^2\rho^2}}\frac{2(1+K)a_2 y}{\Omega_{SD}\rho^2(a_2 - a_1 y)^3} \tag{49}$$

Substituting $a = \sqrt{2K}$, we get,

$$f_Y\left(y\right) = \frac{2(1+K)a_2 y}{\Omega_{SD}\rho^2(a_2 - a_1 y)^3} e^{-\left[\frac{2K}{2}+\frac{(1+K)y^2}{\Omega_{SD}(a_2 - a_1 y)^2\rho^2}\right]} \cdot \sum_{l=0}^{\infty}\frac{1}{(l!)^2}\left[-\left(\frac{K(1+K)y^2}{\Omega_{SD}(a_2 - a_1 y)^2\rho^2}\right)^k\right] \tag{50}$$

$$f_B\left(y\right) = \frac{2(K+1)a_2 y}{\Omega_{SD}\rho^2(a_2 - a_1 y)^3} e^{\left(-\left[K+\frac{(K+1)y^2}{\Omega_{SD}(a_2 - a_1 y)^2\rho^2}\right]\right)} \cdot \sum_{l=0}^{\infty}\frac{1}{(l!)^2}\left(\frac{K\left(K+1\right)y^2}{\Omega_{SD}\left(a_2 - a_1 y\right)^2\rho^2}\right)^l \tag{51}$$

Therefore, the closed-form expression for the OP of signal x_2 at U2 using MRC is as follows after substituting $F_A\left(\gamma_{th} - y\right)$ and $f_B\left(y\right)$ in (31)

$$OPMRC = \int_0^{\gamma_{th}}\left(1 - Q_1\left(\sqrt{2K}, \sqrt{\frac{2\left(1+K\right)}{\Omega_{RD}}\frac{\left(\gamma_{th} - y\right)}{\rho}}\right)\right) \cdot \frac{\left(K+1\right)a_2 2y}{\Omega_{SD}\rho^2(a_2 - a_1 y)^3}\exp\left(-\left[K + \frac{\left(K+1\right)y^2}{\Omega_{SD}\left(a_2 - a_1 y\right)^2\rho^2}\right]\right) \cdot \sum_{l=0}^{\infty}\frac{1}{(l!^2)}\left(\frac{K\left(K+1\right)y^2}{\Omega_{SD}\left(a_2 - a_1 y\right)^2\rho^2}\right)^l dy \tag{52}$$

Substituting (28) with (29), (37) and (52), the final expression for OP using MRC is given as

$$R_{OPMRC} = \left(1 - Q_1\left(\sqrt{2K}, \sqrt{\frac{2(1+K)}{\Omega_{SR}}\frac{\gamma_{th}}{(a_2 - a_1\gamma_{th})\rho}}\right)\right) \left(1 - Q_1\left(\sqrt{2K}, \sqrt{\frac{2(1+K)}{\Omega_{SD}}\frac{\gamma_{th}}{(a_2 - a_1\gamma_{th})\rho}}\right)\right) + Q_1\left(\sqrt{2K}, \sqrt{\frac{2(1+K)}{\Omega_{SR}}\frac{\gamma_{th}}{(a_2 - a_1\gamma_{th})\rho}}\right)\cdot OPMRC \tag{53}$$

The OP for the decoding signal x_2 at U2, using the SC approach at the destination, is provided as

$$OPSC = Pr\left(max\left(\gamma_{2,2}^{[2]}, \gamma_{2,2}^{[1]}\right) < \gamma_{th}\right) \tag{54}$$

$$= Pr\left(\gamma_{2,2}^{[2]} < \gamma_{th}\right) Pr\left(\gamma_{2,2}^{[1]} < \gamma_{th}\right) \tag{55}$$

Equation (56) can be obtained with the help of (35), (37) and (55) as follows

$$OPSC = \left(1 - Q_1\left(\sqrt{2K}, \sqrt{\frac{2(1+K)}{\Omega_{RD}}\frac{\gamma_{th}}{\rho}}\right)\right) \left(1 - Q_1\left(\sqrt{2K}, \sqrt{\frac{2(1+K)}{\Omega_{SD}}\frac{\gamma_{th}}{(a_2 - a_1\gamma_{th})\rho}}\right)\right) \tag{56}$$

substituting (28) with (29), (37) and (56), the final expression for OP using SC is obtained as

$$R_{OPSC} = \left(1 - Q_1\left(\sqrt{2K}, \sqrt{\frac{2(1+K)}{\Omega_{SR}}\frac{\gamma_{th}}{(a_2 - a_1\gamma_{th})\rho}}\right)\right) \left(1 - Q_1\left(\sqrt{2K}, \sqrt{\frac{2(1+K)}{\Omega_{SD}}\frac{\gamma_{th}}{(a_2 - a_1\gamma_{th})\rho}}\right)\right) + Q_1\left(\sqrt{2K}, \sqrt{\frac{2(1+K)}{\Omega_{SR}}\frac{\gamma_{th}}{(a_2 - a_1\gamma_{th})\rho}}\right)\cdot OPSC \tag{57}$$

C. IMPERFECT SIC ANALYSIS

In order to account for the interference that remains after cancellation, a residual interference factor ξ is included to describe incomplete SIC. Since the outage analysis of the far user is the main topic of this article, residual interference is typically zero because SIC is not necessary at the far user unless there is interference from a prior decoding layer. However, by assuming that the DF user relays the distant user's signal in addition to its own, a residual interference component scaled by ξ from the near DF user (U1) can be included.

The SINR of the distant user's signal x_2 after receiving this signal at U2 is expressed as

$$\gamma_{2,2}^{[2]} = \frac{|h_{12}|^2 P_{\text{tx}}}{\xi|h_{12}|^2 P_{\text{tx}} + \sigma^2}, \tag{58}$$

This can be expressed in normalised form as

$$\gamma_{2,2}^{[2]} = \frac{|h_{12}|^2\rho}{\xi|h_{12}|^2\rho + 1}, \tag{59}$$

Since the relay-destination link incorporates residual interference, the relevant outage probability is provided by

$$\Pr\left(\gamma_{2,2}^{[2]} < \gamma_{\rm th}\right) = \Pr\left(|h_{12}|^2 < \frac{\gamma_{\rm th}}{(1 - a_2\xi\gamma_{\rm th})\rho}\right) \tag{60}$$

Substituting this result into (33), the CDF can be expressed as

$$F_A(x) = 1 - Q_1\left(\sqrt{2K}, \sqrt{\frac{2(1+K)}{\Omega_{\rm RD}}\frac{\gamma_{\rm th}}{(1 - a_2\xi\gamma_{\rm th})\rho}}\right), \tag{61}$$

where $Q_1(\cdot,\cdot)$ denotes the first-order Marcum Q-function.

By substituting this expression into (31), the outage probability of U2 under MRC at the destination is obtained. Similarly, the outage probability under SC is derived by substituting this result into (55).

D. IMPERFECT CSI MODEL

By assuming estimated channel conditions, the same analysis can be extended by taking imperfect channel state information (CSI) into consideration. It is feasible to model a Rician fading channel's estimated channel coefficient as [42]

$$\hat{h} = (1 - \delta^2)h + \delta v, \tag{62}$$

where δ^2 is the channel estimation error variance, h is the true channel, $\hat{h}$ is the estimated channel, and v is the estimation noise term [20].

For a simplified imperfect-CSI model, when the estimation noise variance σ_v^2 is equal to the scattered component variance σ_w^2, the estimated scattered variance becomes

$$\hat{\sigma}_h^2 = \sigma_w^2 \tag{63}$$

Consequently, the Rician K-factor is reduced to

$$\hat{K} = (1 - \delta^2)K \tag{64}$$

Therefore, the OP expressions can be obtained by substituting K with $(1 - \delta^2)K$ in (53) and (57).

E. INTUITION AND ASYMPTOTIC BEHAVIOR OF MRC VERSUS SC

At high SNR ($\rho \to \infty$), the argument of the CDF approaches zero. For i.i.d. Rician fading branches with diversity order B, the CDF behaves as

$$F_G(x) = Cx^B, \quad x \to 0, \tag{65}$$

where

$$C = \frac{1+K}{\Omega}e^{-K} \tag{66}$$

For MRC with two independent branches, the OP can be approximated as [20]

$$\Pr(h_{\rm SD} + h_{\rm RD} < x) \sim \frac{C^2}{2}x^2 \tag{67}$$

From (24) and (26), at high SNR,

$$x = \frac{\gamma_{\rm th}}{(a_2 - a_1\gamma_{\rm th})\rho} \tag{68}$$

Substituting in (67) expression yields

$$\Pr(h_{\rm SD} + h_{\rm RD} < x) \sim \frac{C^2}{2}\left(\frac{\gamma_{\rm th}}{(a_2 - a_1\gamma_{\rm th})\rho}\right)^2 \sim C_{\rm MRC}\rho^{-2} \tag{69}$$

For SC, since the links are independent,

$$\Pr(h_{\rm SD} < x, h_{\rm RD} < x) \sim C^2x^2 \tag{70}$$

Substituting x gives

$$\Pr(h_{\rm SD} < x, h_{\rm RD} < x) \sim C^2\left(\frac{\gamma_{\rm th}}{(a_2 - a_1\gamma_{\rm th})\rho}\right)^2 \sim C_{\rm SC}\rho^{-2} \tag{71}$$

Comparing (69) and (71),

$$C_{\rm MRC} < C_{\rm SC} \tag{72}$$

F. CAPACITY INSIGHTS

The ergodic capacity at high SNR can be expressed as

$$C(\rho) = \log_2\rho + \mathbb{E}[\log_2 G] + o(1), \tag{73}$$

with G being the channel power gain. This shows that MRC yields a strictly larger high-SNR constant than SC [43]. At low SNR, the capacity can be approximated as

$$C(\rho) \approx \frac{\rho\,\mathbb{E}[G]}{\ln 2}, \tag{74}$$

which again favors MRC since it aggregates energy across multiple diversity branches.

G. AVERAGE BER

The BER is the percentage of bits that are sent incorrectly because of interference, noise, or other issues. BER is a performance metric used in digital communications to evaluate how well the recipient decodes the transmitted data. The BER can be calculated by assessing the probability that a bit would be incorrectly received due to noise. To find the error probability, differential modulation is taken into consideration and use the BER formula. The error probability is given as

$$P_e = aE\left[Q\sqrt{bSINR}\right] \tag{75}$$

where the values of a and b will specify the modulation technique type [44]. Let γ_{th} represent the $SINR$.

$$P_e = aE\left[Q\sqrt{b\gamma_{th}}\right] \tag{76}$$

By applying the mathematical definition of the Expectation notation, we get

$$P_e = a\int_0^\infty Q(\sqrt{b\gamma_{th}})dF_\gamma(\gamma_{th}) \tag{77}$$

Assuming differential modulation schemes and using the Moment Generating Function (MGF) of Nakagami-m fading channel [44], the equation for BER is given as follows

$$P_e = \frac{a^b}{2\sqrt{2\pi}\Gamma(b)} \int_0^\infty \exp\left(-\frac{b\gamma_{th}}{2}\right) {\gamma_{th}}^{a-1} F_\gamma(\gamma_{th})\, d\gamma_{th} \tag{78}$$

Since

$$F_\gamma(\gamma_{th}) = \begin{cases} P\left(\gamma < \frac{\gamma_{th}}{a_2 - a_1\gamma_{th}}\right), & 0 \le \gamma_{th} < \frac{a_2}{a_1} \\ 0, & \gamma_{th} \ge \frac{a_2}{a_1} \end{cases}$$

Let $au = \frac{a_2}{a_1}$. The integral limits reduce from 0 to au and consequently, the estimated BER value can be provided as

$$P_e \approx \frac{a^b}{2\sqrt{2\pi}\Gamma(b)} \left[\int_0^{a_u} \exp\left(-\frac{b\gamma_{th}}{2}\right) {\gamma_{th}}^{a-1} F_\gamma(\gamma_{th})\, d\gamma_{th}\right] \tag{79}$$

For Differential Phase Shift Keying (DPSK) modulation, choosing $a = b = 1$ and replacing, $t = \frac{2\gamma_{th}}{a_u} - 1$, where, $\gamma_{th} = (t+1)\frac{a_u}{2}$ in (45)

$$P_e \approx \frac{1}{2\sqrt{2\pi}} \left[\frac{a_u}{2}\int_{-1}^{1} \exp\left(-\frac{a_u(t+1)}{4}\right) F_\gamma\left(\frac{a_u(t+1)}{2}\right) dt\right] \tag{80}$$

For U2, the average BER for MRC can be found using Chebyshev-Gauss quadrature from [45] and [46] as

$$P_{e2MRC} \approx \frac{1}{2\sqrt{2\pi}} \left[\frac{\alpha_u}{2} \sum_{i=1}^{u1} \bar{w} \exp\left(-\frac{a_u(t_i+1)}{4}\right) F_{\gamma MRC}\left(\frac{a_u(t_i+1)}{2}\right)\sqrt{1-{t_i}^2}\right] \tag{81}$$

where $\bar{w} = \frac{\pi}{u1}$, $t_i = \cos\frac{(2i-1)\pi}{2u1}$, $F_{\gamma MRC}(\gamma_{th}) = R_{OPMRC}$ Similarly, the average BER for U2 may be found as follows when the SC method is used at the destination

$$P_{e2SC} \approx \frac{1}{2\sqrt{2\pi}} \left[\frac{\alpha_u}{2} \sum_{i=1}^{u1} \bar{w}\, exp\left(-\frac{a_u(t_i+1)}{4}\right) F_{\gamma SC}\left(\frac{a_u(t_i+1)}{2}\right)\sqrt{1-{t_i}^2}\right] \tag{82}$$

solving (82) by substituting $F_{\gamma SC}(\gamma_{th}) = R_{OPSC}$ in the equation, plotting of the behavior of average BER is possible.

H. ERGODIC CAPACITY

The equation for capacity is given as

$$C = \frac{1}{2}\log(1+SNR) \tag{83}$$

TABLE 1. Simulation parameters.

Parameter	Values
Power coefficient of U2, a_2	0.9, 0.8, 0.7
Power coefficient of U1, a_1	0.1, 0.2, 0.3
Variance σ^2	1
Scale parameters, $\Omega_{SR} = \Omega_{RD} = \Omega_{SD}$	1
Number of points, u_1	100
Threshold SNR, γ_{th}	1 Mbps
Rician parameter K factor, K	1, 2, 3
Residual interference factor ξ	0, 0.05, 0.01
Channel estimation error variance δ^2	0, 0.05, 0.1

The ergodic capacity is given by the expression [42]

$$Er = \int_0^\infty f_\gamma(\gamma_{th})\log(1+\gamma_{th})d\gamma_{th} \tag{84}$$

Equation (84) then simplifies to

$$Er = \frac{1}{\ln(2)}\int_0^\infty \frac{1-F_\gamma(\gamma_{th})}{1+\gamma_{th}} d\gamma_{th} \tag{85}$$

Hence, the approximated expression can be obtained after simplification as

$$Er = \log_2(1+au) - \frac{au}{2\ln(2)}\int_{-1}^{1} \frac{F_\gamma(\gamma_{th})}{1+\frac{au}{2}(t+1)} dt \tag{86}$$

Using the Chebyshev-Gauss quadrature [46], the ergodic capacity at U2 can be obtained as

$$Er = \log_2(1+au) - \frac{au}{2\ln(2)}\sum_{i=1}^{u1} \bar{w}\, F_\gamma\left(\frac{a_u(t_i+1)}{2}\right) \cdot \frac{1}{1+\frac{au}{2}(t_i+1)}\sqrt{1-{t_i}^2} \tag{87}$$

The ergodic capacity for the MRC and SC techniques is then visualised by substituting (52) and (56) in (87), respectively.

IV. RESULTS AND DISCUSSIONS

In a DF NOMA-based system, the OP of far end user U2 is shown in Figure 2 assuming a Rician fading channel. The simulation results were obtained by choosing the target rate γ_{th} as 1Mbps. The power coefficients are chosen as fixed values of $a_2 = 0.8$ and $a_1 = 0.2$ and $\Omega_{SR} = \Omega_{RD} = 1, \Omega_{SD} = 1, \sigma = 1, u1 = 100$. In Figure 2., it has been noticed that the proposed NOMA system performs better when the destination employs the MRC strategy than when the destination employs the SC technique. The OP results for Rician factor K = 0, 1, and 3 are plotted. When the value of K increases, the outage also reduces drastically for MRC. Using the SC method, as K is increased, the OP values reduce slightly compared to MRC. In Figure 3, the theoretically derived results of OP are then compared with the outcomes of a Monte Carlo simulation. This is based on 10^5 trails with $a_2 = 0.8$ and $a_1 = 0.2$ and threshold value of γ_{th} as 1Mbps. This demonstrates that the outcomes align with the theoretical assessment.

Figure 4. illustrates the BER simulation findings by taking the target rate, power coefficients, the Rician factor, and

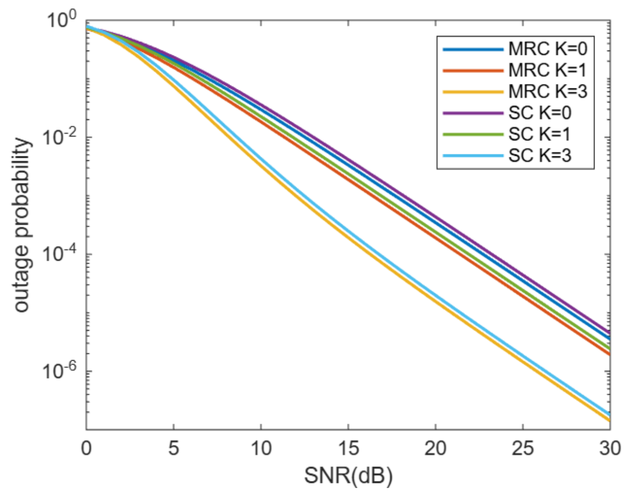

FIGURE 2. OP of the U2 for $\gamma_{th} = 1$ with Rician Factor (K) = 0,1,3 for both MRC and SC.

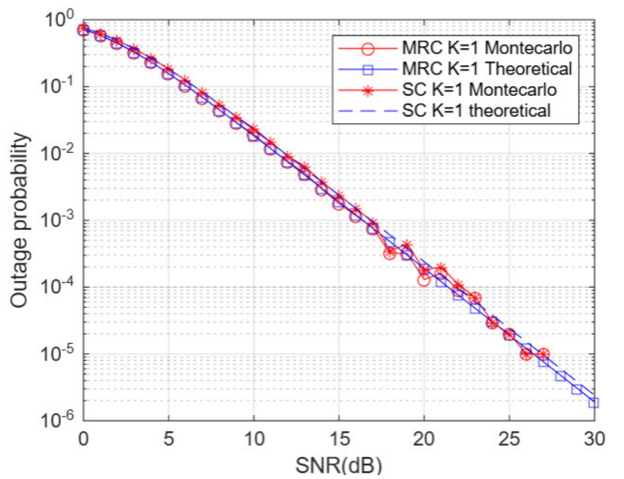

FIGURE 3. Comparison of OP of Monte Carlo simulation for $\gamma_{th} = 1$ and K = 1 for both MRC and SC with theoretical expression.

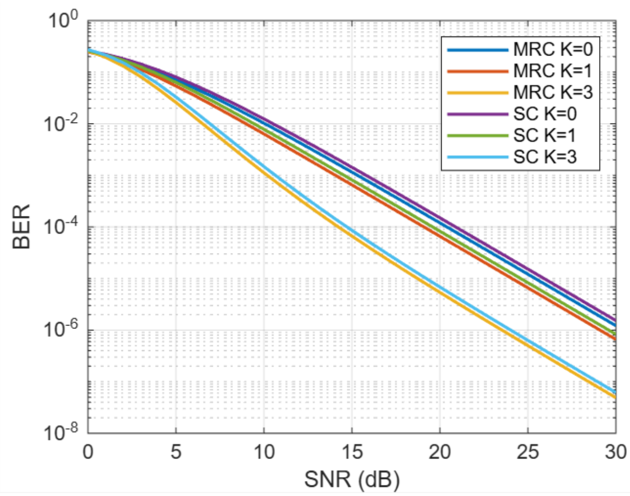

FIGURE 4. BER for $\gamma_{th} = 1$with Rician factor (K) = 0,1,3 for both MRC and SC.

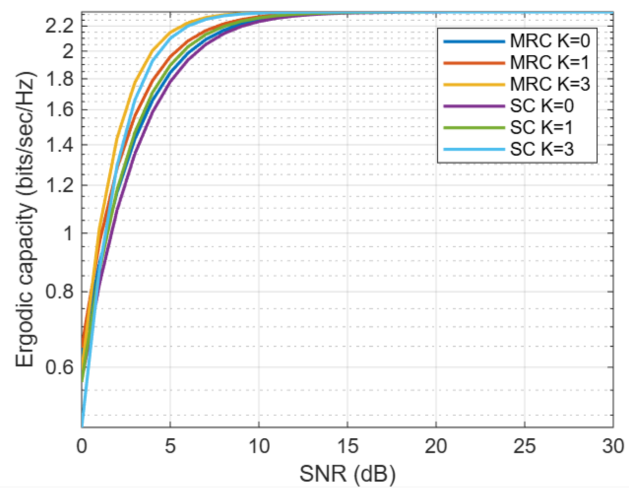

FIGURE 5. Ergodic capacity for $\gamma_{th} = 1$ with Rician factor (K) = 0,1,3 for both MRC and SC.

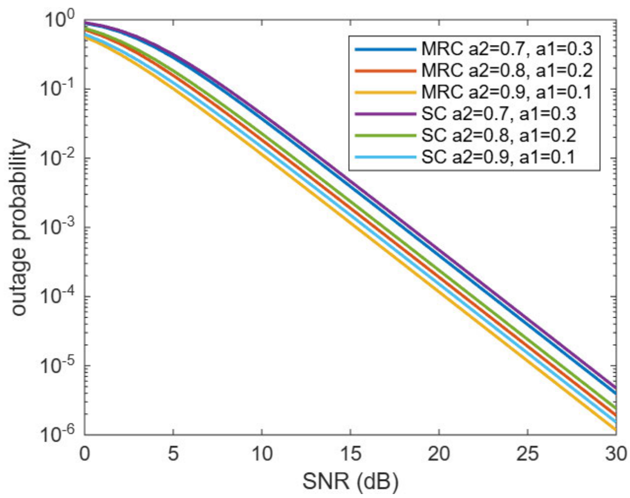

FIGURE 6. OP for U2 with $\gamma_{th} = 1$ for varying power coefficients where $a_2 = 0.9, 0.8, 0.7$.

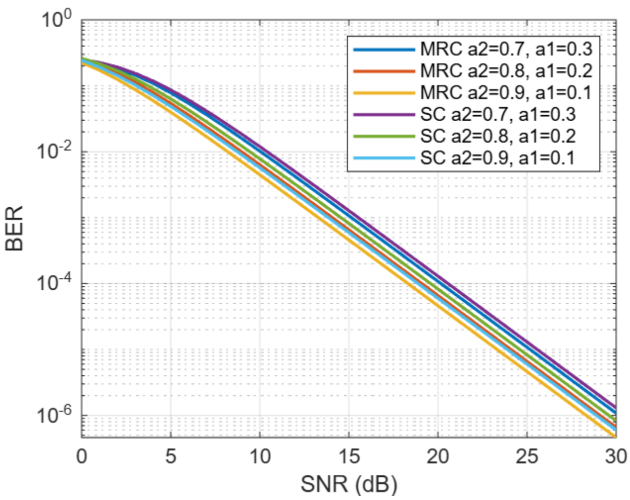

FIGURE 7. BER for users with $\gamma_{th} = 1$ for varying power coefficients where $a_2 = 0.9, 0.8, 0.7$.

the variances values considered for the analysis of OP. The plot demonstrates how the MRC method lowers the BER till around 10^{-6} at 30 dB for K = 0 and the value becomes lower of about 10^{-7} at 30 dB for K = 3. In SC technique, it reduces to a value of around 10^{-6} at 30 dB for K = 0 and goes lower

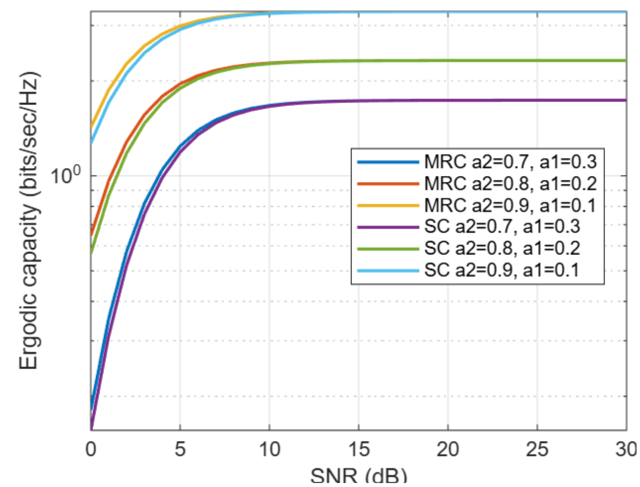

FIGURE 8. Ergodic capacity for $\gamma_{th} = 1$ for varying power coefficients where $a_2 = 0.9, 0.8, 0.7$.

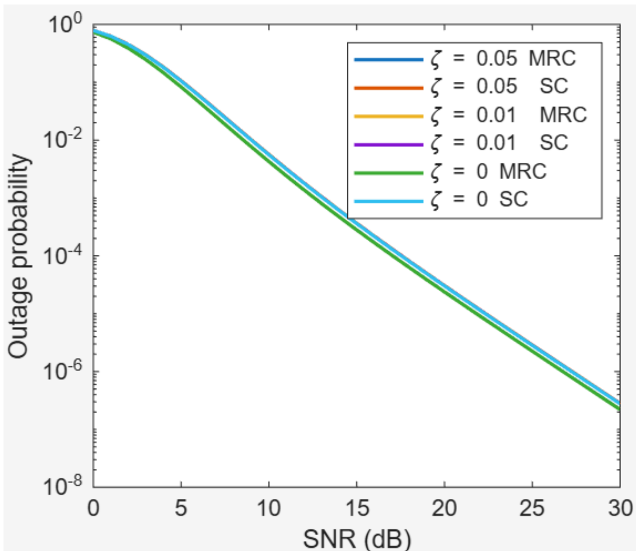

FIGURE 9. OP for $\delta^2 = 0.1$ for varying ζ values of = 0, 0.01, 0.05.

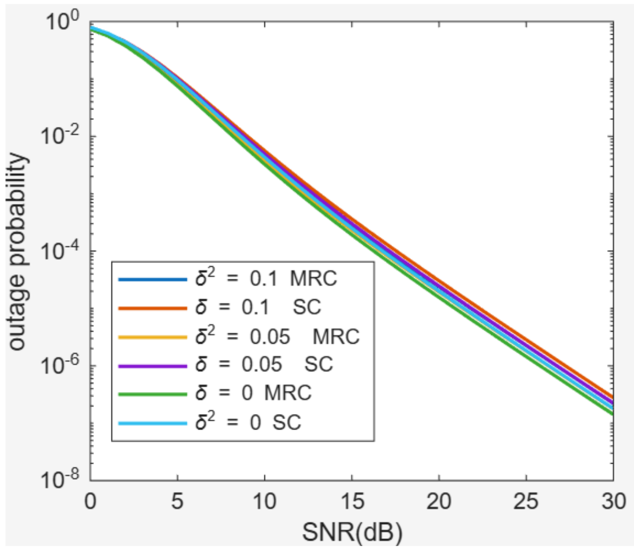

FIGURE 10. OP for $\zeta = 0.01$ for varying δ^2 values of = 0, 0.05, 0.1.

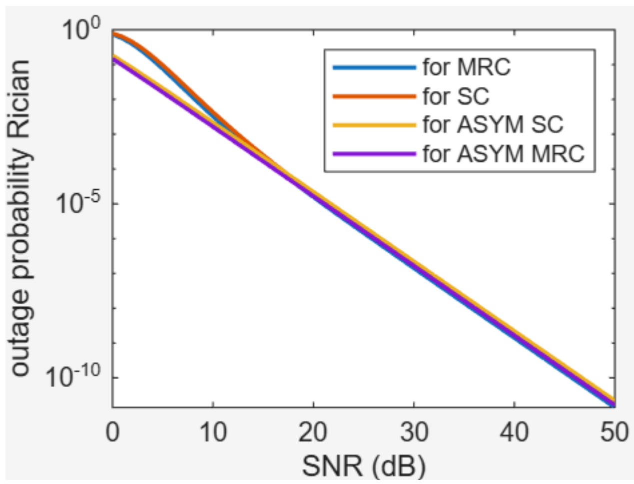

FIGURE 11. OP for K = 3, at $a_2 = 0.8$ and $a_1 = 0.2$.

than 10^{-7} for K = 3. It can be seen that BER using MRC outperforms SC. As K is increasing due to the increase in LOS component, the BER is also improved. Figure 5. shows the ergodic capacity of the U2 for the same values of parameters as in OP and BER. Using SC method, initially at low SNRs the ergodic rate tends to increase from 0 bits/sec/Hz to a constant value of 2.3 bits/sec/Hz after 12 dB. Whereas for MRC technique, the ergodic capacity increases from 0.2 bits/sec/Hz to a constant value of 2.3 bits/sec/Hz after 10 dB SNR. It is observed from the results that MRC provides better capacity than SC at low SNRs. Whereas at high SNRs it remains the same. The ergodic capacity is also improved with an increase in Rice factor.

Figure 6. and Figure 7. shows the OP and BER for the change in power coefficient allocated to the users for K = 1. It is noticed that as power is increased, the OP and BER are also improved for both cases of MRC and SC techniques. Figure 8. shows the ergodic capacity for MRC and SC with varying power allocation coefficients where it achieves a maximum value of 3.2 bits/sec/Hz. Hence, the user with the better power coefficient exhibits better overall performance in a NOMA network providing fairness to the far user that has weak channel conditions.

To show the impact of imperfect SIC at the destination a plot for OP at K = 3 and $a_2 = 0.8$ and $a_1 = 0.2$ is shown in Figure 9. This is plotted by considering the imperfect CSI where $\delta^2 = 0.1$, while varying $\zeta = 0, 0.01, 0.05$. Figure 10 show the plot for OP by keeping ζ constant at 0.01 while varying δ^2 as 0, 0.05, 0.1. From the plots, it illustrate that the OP increases with the inclusion of residual factor and channel estimation error factor. The high SNR approximations plot of OP are also included in Figure 11., for K = 3, $a_2 = 0.8$ and $a_1 = 0.2$, which shows the parallel slopes and constant SNR gap between MRC and SC. The SNR gap is computed at OP level of 10^{-3} is around 0.65 dB. This gap is primarily due to the different coding gains of the two combining techniques

TABLE 2. Performance comparison of MRC and SC under varying conditions.

Performance Metric	Combining Technique	Variation with K	Effect of a_2/a_1
Outage Probability	MRC	The value decreases as K increases. It achieves the lowest value of 1.4×10^{-7} at 30 dB.	A higher value of a_2 gives better performance. The outage at $a_2 = 0.7$ behaves similar to the outage at SC for $a_2 = 0.9$.
	SC	The value also improves with the increase in K. Its lowest value is 1.7×10^{-7} at 30 dB.	Provides better performance for higher values of a_2, but underperforms compared to MRC.
BER	MRC	As K increases, the performance improves. The lowest value achieved is 10^{-8} at 30 dB.	As a_2 decreases, the BER increases. Better performance is observed at 30 dB with a value of 4.6×10^{-7}.
	SC	Improves as K is increased, also attains a value closer to 10^{-8} at 30 dB but higher than MRC.	Improves with the increase in a_2 value. Compared to MRC, SC underperforms for the same a_2 values.
Ergodic Capacity	MRC	The value for $K = 3$ is higher than for $K = 1$ and $K = 0$.	MRC with high values of power coefficient a_2 gives better capacity than with lower values of a_2.
	SC	The plot for $K = 0$ has a lower value compared to higher values of K.	MRC outperforms SC. However, SC shows better results for higher values of a_2.

used which is reflected in (69) and (71). Relaying error at the DF user also contributes to this gap.

These results imply that the CNOMA technology can help in enhancing the connectivity, and reliability and provide better coverage area in future satellite communication. As in the proposed model, the user acts as a relay strengthening the weak users in remote areas and providing better coverage. Table 2 shows the summary of results obtained from the graph.

V. CONCLUSION

In this work, we presented a comprehensive performance analysis of a CNOMA system incorporating DF relaying with two diversity combining techniques, MRC and SC over Rician fading channels in satellite communications. Key performance indicators, such as ergodic capacity, average BER, and OP, were computed analytically and verified using Monte Carlo simulations. The findings showed that MRC performs noticeably better than SC in terms of achievable ergodic capacity, BER, and OP. Notably, performance gains of MRC increase substantially with stronger LOS conditions indicated by higher Rician factor values. Additionally, optimal power allocation was shown to enhance system performance, improving fairness for far users under weaker channel conditions. The presented results clearly demonstrate that the MRC technique significantly outperforms the SC technique in terms of OP, BER, and achievable ergodic capacity. The superiority of MRC is particularly notable in scenarios with stronger LoS components, as indicated by higher values of the Rician factor (K). Additionally, optimal power allocation was shown to enhance overall system performance, providing improved fairness to far users experiencing weaker channel conditions. Overall, this research confirms the effectiveness of cooperative NOMA in improving satellite communication systems' performance, laying a foundation for future studies to further address identified challenges and advance robust, secure next-generation satellite networks. In order to facilitate analytical derivation, perfect CSI is assumed at the receivers. Future research may examine the effect of CSI estimate errors on system performance.

This study explicitly addresses existing research gaps by integrating user-aided cooperative relaying and diversity techniques within a satellite communication environment, an area previously unexplored in the literature. However, several limitations remain and open new avenues for future research. For instance, our current model does not address the critical issue of physical-layer security, which is inherently vulnerable in cooperative communication systems due to potential eavesdropping. Future investigations should consider integrating robust physical-layer security measures such as cooperative jamming or secure beamforming techniques.

REFERENCES

[1] N. Ye, H. Han, L. Zhao, and A.-H. Wang, "Uplink nonorthogonal multiple access technologies toward 5G: A survey," *Wireless Commun. Mobile Comput.*, vol. 2018, no. 1, Jan. 2018, Art. no. 6187580.

[2] D.-T. Do and C.-B. Le, "Application of NOMA in wireless system with wireless power transfer scheme: Outage and ergodic capacity performance analysis," *Sensors*, vol. 18, no. 10, p. 3501, Oct. 2018.

[3] K. M. Rabie, B. Adebisi, E. H. G. Yousif, H. Gacanin, and A. M. Tonello, "A comparison between orthogonal and non-orthogonal multiple access in cooperative relaying power line communication systems," *IEEE Access*, vol. 5, pp. 10118–10129, 2017.

[4] Z. Ding, X. Lei, G. K. Karagiannidis, R. Schober, J. Yuan, and V. K. Bhargava, "A survey on non-orthogonal multiple access for 5G networks: Research challenges and future trends," *IEEE J. Sel. Areas Commun.*, vol. 35, no. 10, pp. 2181–2195, Oct. 2017.

[5] A. Ahmed, X. Wang, A. Hawbani, W. Yuan, H. Tabassum, Y. Liu, M. U. F. Qaisar, Z. Ding, N. Al-Dhahir, A. Nallanathan, and D. W. K. Ng, "Unveiling the potential of NOMA: A journey to next-generation multiple access," *IEEE Commun. Surveys Tuts.*, vol. 27, no. 5, pp. 3099–3164, Oct. 2025.

[6] M. Shirvanimoghaddam, M. Dohler, and S. J. Johnson, "Massive non-orthogonal multiple access for cellular IoT: Potentials and limitations," *IEEE Commun. Mag.*, vol. 55, no. 9, pp. 55–61, Sep. 2017.

[7] Z. Ding, Y. Liu, J. Choi, Q. Sun, M. Elkashlan, I. Chih-Lin, and H. V. Poor, "Application of non-orthogonal multiple access in LTE and 5G networks," *IEEE Commun. Mag.*, vol. 55, no. 2, pp. 185–191, Feb. 2017.

[8] S. M. R. Islam, N. Avazov, O. A. Dobre, and K.-S. Kwak, "Power-domain non-orthogonal multiple access (NOMA) in 5G systems: Potentials and challenges," *IEEE Commun. Surveys Tuts.*, vol. 19, no. 2, pp. 721–742, 2nd Quart., 2017.

[9] R. Thirunavukkarasu and R. Balasubramanian, "An efficient code domain NOMA scheme with enhanced spectral and energy efficiency for networks beyond 5G," *Wireless Pers. Commun.*, vol. 120, no. 1, pp. 353–377, Sep. 2021.
[10] J. Li, Y. Peng, Y. Yan, X.-Q. Jiang, H. Hai, and M. Zukerman, "Cognitive radio network assisted by OFDM with index modulation," *IEEE Trans. Veh. Technol.*, vol. 69, no. 1, pp. 1106–1110, Jan. 2020.
[11] T. M. Cover, *Elements of Information Theory*. Hoboken, NJ, USA: Wiley, 1999.
[12] K. Ashwini and V. K. Jagadeesh, "Co-operative non-orthogonal multiple access networks: A survey," *World J. Eng.*, vol. 21, no. 6, pp. 1128–1141, Dec. 2024.
[13] X. Zhang and M. Haenggi, "The performance of successive interference cancellation in random wireless networks," *IEEE Trans. Inf. Theory*, vol. 60, no. 10, pp. 6368–6388, Oct. 2014.
[14] T. M. Cover, "Broadcast channels," *IEEE Trans. Inf. Theory*, vol. IT-18, no. 1, pp. 2–14, Jan. 1972.
[15] S. Ahmad and M. J. Khan, "Ergodic secrecy capacity of cooperative NOMA system with untrusted user," *Wireless Pers. Commun.*, vol. 133, no. 1, pp. 181–198, Nov. 2023.
[16] İ. Baştürk, Y. Chen, and M.-S. Alouini, "Energy-efficient communication for user-relay aided cellular networks with OFDMA," *Phys. Commun.*, vol. 33, pp. 153–164, Apr. 2019.
[17] G. Levin and S. Loyka, "Amplify-and-forward versus decode-and-forward relaying: Which is better?" in *Proc. 22th Int. Zurich seminar Commun. (IZS)*, 2012, pp. 123–126.
[18] K. Zheng, J. Fu, and X. Liu, "Relay selection and deployment for NOMA-enabled multi-AAV-assisted WSN," *IEEE Sensors J.*, vol. 25, no. 9, pp. 16235–16249, May 2025.
[19] Z. Ding, M. Peng, and H. V. Poor, "Cooperative non-orthogonal multiple access in 5G systems," *IEEE Commun. Lett.*, vol. 19, no. 8, pp. 1462–1465, Aug. 2015.
[20] M. K. Simon and M.-S. Alouini, *Digital Communication Over Fading Channels*. Hoboken, NJ, USA: Wiley, 2004.
[21] J. G. Proakis and M. Salehi, *Digital Communications*, vol. 4. New York, NY, USA: McGraw-Hill, 2001.
[22] G. K. Karagiannidis, D. A. Zogas, N. C. Sagias, S. A. Kotsopoulos, and G. S. Tombras, "Equal-gain and maximal-ratio combining over nonidentical Weibull fading channels," *IEEE Trans. Wireless Commun.*, vol. 4, no. 3, pp. 841–846, May 2005.
[23] M. Akbari, M. R. Manesh, A. A. El-Saleh, and A. W. Reza, "Receiver diversity combining using evolutionary algorithms in Rayleigh fading channel," *Sci. World J.*, vol. 2014, pp. 1–11, Jun. 2014.
[24] K. An, X. Yan, T. Liang, and W. Lu, "NOMA based satellite communication networks: Architectures, techniques and challenges," in *Proc. IEEE 19th Int. Conf. Commun. Technol. (ICCT)*, Oct. 2019, pp. 1105–1110.
[25] I. Khan, "Performance analysis of 5G cooperative-NOMA for IoT-intermittent communication," *Int. J. Commun. Netw. Inf. Secur. (IJCNIS)*, vol. 9, no. 3, pp. 314–322, Apr. 2022.
[26] R. Jiao, L. Dai, J. Zhang, R. MacKenzie, and M. Hao, "On the performance of NOMA-based cooperative relaying systems over Rician fading channels," *IEEE Trans. Veh. Technol.*, vol. 66, no. 12, pp. 11409–11413, Dec. 2017.
[27] P. Tran Tin, V.-D. Phan, D. Si Thien Chau, T. N. Nguyen, and P. X. Nguyen, "Performance analysis in DF energy harvesting full-duplex relaying network with MRC and SC at the receiver under impact of eavesdropper," *J. Electr. Comput. Eng.*, vol. 2021, pp. 1–9, Jun. 2021.
[28] V. Singh, V. Bankey, and P. K. Upadhyay, "Underlay cognitive hybrid satellite-terrestrial networks with cooperative-NOMA," in *Proc. IEEE Wireless Commun. Netw. Conf. (WCNC)*, May 2020, pp. 1–6.
[29] Q. Li, M. El-Hajjar, C. Xu, J. An, C. Yuen, and L. Hanzo, "Stacked intelligent metasurfaces for holographic MIMO-aided cell-free networks," *IEEE Trans. Commun.*, vol. 72, no. 11, pp. 7139–7151, Nov. 2024.
[30] Q. Li, M. El-Hajjar, Y. Sun, and L. Hanzo, "Performance analysis of reconfigurable holographic surfaces in the near-field scenario of cell-free networks under hardware impairments," *IEEE Trans. Wireless Commun.*, vol. 23, no. 9, pp. 11972–11984, Sep. 2024.
[31] Q. Li, M. El-Hajjar, K. Cao, C. Xu, H. Haas, and L. Hanzo, "Holographic metasurface-based beamforming for multi-altitude LEO satellite networks," *IEEE Trans. Wireless Commun.*, vol. 24, no. 4, pp. 3103–3116, Apr. 2025.
[32] Z. Ding, F. Adachi, and H. V. Poor, "The application of MIMO to non-orthogonal multiple access," *IEEE Trans. Wireless Commun.*, vol. 15, no. 1, pp. 537–552, Jan. 2016.
[33] L. Dai, B. Wang, Z. Ding, Z. Wang, S. Chen, and L. Hanzo, "A survey of non-orthogonal multiple access for 5G," *IEEE Commun. Surveys Tuts.*, vol. 20, no. 3, pp. 2294–2323, 3rd Quart., 2018.
[34] S. Yang, S. Mao, and B. Tan, "Closed-form solution for the max-min fairness problem in non-orthogonal multiple access systems," *Int. J. Cognit. Comput. Eng.*, vol. 2, pp. 191–195, Jun. 2021.
[35] S. Shi, L. Yang, and H. Zhu, "Outage balancing in downlink nonorthogonal multiple access with statistical channel state information," *IEEE Trans. Wireless Commun.*, vol. 15, no. 7, pp. 4718–4731, Jul. 2016.
[36] S. Jonqyin and I. S. Reed, "Performance of MDPSK, MPSK, and noncoherent MFSK in wireless Rician fading channels," *IEEE Trans. Commun.*, vol. 47, no. 6, pp. 813–816, Jun. 1999.
[37] B. H. Liu, B. P. Otis, S. Challa, P. Axon, C. T. Chou, and S. K. Jha, "The impact of fading and shadowing on the network performance of wireless sensor networks," *Int. J. Sensor Netw.*, vol. 3, no. 4, pp. 211–223, 2008.
[38] Q. T. Zhang and D. P. Liu, "A simple capacity formula for correlated diversity Rician fading channels," *IEEE Commun. Lett.*, vol. 6, no. 11, pp. 481–483, Nov. 2002.
[39] C. Xiao, Y. R. Zheng, and N. C. Beaulieu, "Statistical simulation models for Rayleigh and Rician fading," in *Proc. IEEE Int. Conf. Commun.*, vol. 5, Sep. 2003, pp. 3524–3529.
[40] I. Ghareeb and D. Tashman, "Statistical analysis of cascaded Rician fading channels," *Int. J. Electron. Lett.*, vol. 8, no. 1, pp. 46–59, Jan. 2020.
[41] I. S. Gradshteyn and I. M. Ryzhik, *Table of Integrals, Series, and Products*. New York, NY, USA: Academic, 2014.
[42] A. Goldsmith, *Wireless Communications*. Cambridge, U.K.: Cambridge Univ. Press, 2005.
[43] D. Tse and P. Viswanath, *Fundamentals of Wireless Communication*. Cambridge, U.K.: Cambridge Univ. Press, 2005.
[44] T.-A. Nguyen, H.-V. Nguyen, D.-T. Do, and A. Silva, "Performance analysis of downlink double-IRS systems relying on non-orthogonal multiple access," *IEEE Access*, vol. 11, pp. 110208–110220, 2023.
[45] M. Abramowitz and I. A. Stegun, *Handbook of Mathematical Functions: With Formulas, Graphs, and Mathematical Tables*, vol. 55. Chelmsford, MA, USA: Courier Corporation, 1965.
[46] M. R. Eslahchi, M. Dehghan, and M. Masjed-Jamei, "On numerical improvement of the first kind Gauss–Chebyshev quadrature rules," *Appl. Math. Comput.*, vol. 165, no. 1, pp. 5–21, Jun. 2005.

K. ASHWINI received the B.E. and master's degrees in electronics and communication engineering from Visvesvaraya Technological University, Belgaum, Karnataka, India, in 2009 and 2014, respectively, and the Ph.D. degree from the Department of Electronics and Communication Engineering, Visveswaraya Technological University, in 2025, under the supervision of Dr. V. K. Jagadeesh and Dr. Ashish Singh. Her master's degree specializes in microelectronics and control systems. She is currently an Assistant Professor with the NMAM Institute of Technology, Nitte, India. Her fields of research interests include wireless communication and cooperative communication.

ASHISH SINGH (Member, IEEE) received the B.Tech. degree in applied electronics and instrumentation from Uttar Pradesh Technical University, India, in 2007, and the M.Tech. and Ph.D. degrees in communication technology from the Department of Electronics and Communication Engineering, University of Allahabad (A Central University), in 2009 and 2015, respectively. Currently, he is an Associate Professor with the NMAM Institute of Technology, Nitte, India. He has published more than 40 research papers in different national and international journals and conference proceedings. His areas of research interests include patch antenna, millimeter waves, optical communication, nano antenna, and biomedical instrumentation.

JAGADEESH V. K. (Senior Member, IEEE) received the B.Tech. degree in electronics and communication engineering from Kannur University, Kannur, in 2006, the master's degree in microwave and TV engineering from Kerala University, in 2009, and the Ph.D. degree from the Department of Electronics and Communication Engineering, National Institute of Technology, Tiruchirappalli, in 2016. He is currently an Assistant Professor with the National Institute of Technology Calicut, Kozhikode. His areas of research interests include free space optics, RF/FSO, visible light communication, and wireless communication.

RACHANA SHENOY is currently pursuing the bachelor's degree in electronics and communication engineering with the NMAM Institute of Technology, Nitte, with a strong passion for digital design and embedded systems. She is passionate about understanding the intricacies of embedded systems and programmable devices, developing efficient, real-world solutions through digital circuit design. She aspires to contribute to advancements in embedded technology and digital electronics.

DUSHANTHA NALIN K. JAYAKODY (Senior Member, IEEE) received the M.Sc. degree in electronics and communications engineering from Eastern Mediterranean University, Türkiye, and the Ph.D. degree in electronics and communications engineering from University College Dublin, Ireland, in 2014. From 2014 to 2016, he was a Postdoctoral Research Fellow with the University of Tartu, Estonia, and the University of Bergen, Norway. He held visiting and/or sabbatical positions at the Center for Telecommunications Research, The University of Sydney, Australia, in 2015, and Texas A&M University, in 2018. From 2016 to 2021, he was a Professor with the School of Computer Science and Robotics, National Research Tomsk Polytechnic University (TPU), Russia. He was a Visiting Professor with the Federal University of Juiz de Fora, Brazil, in 2019. He was a Visiting Professor with the University of Jyväskylä, Finland, in 2019 and 2022, within the framework of the Academy of Finland. From 2019 to 2021, he was the Dean of the Faculty of Postgraduate Studies and Research, Sri Lanka Technological Campus, Sri Lanka. From 2019 to 2022, he was a SPARC Professor with the Department of Electronics and Communication Engineering, National Institute of Technology, Tiruchirappalli, India, within the framework of the Ministry of Human Resources in India. From 2021 to 2022, he was the Director of Postgraduate, Research, and Impact at Sri Lanka Technological Campus. From 2021 to 2022, he was with the Department of Engineering and Computer Science/Autonoma TechLab, Universidade Autónoma de Lisboa, Portugal. Since 2022, he has been a Professor with Universidade Lusófona, Portugal. He supervises seven Ph.D. students and five postdoctoral researchers. He is currently supervising five Ph.D. students, one postdoctoral researcher, and many master's and undergraduate students. In his career, so far, he has attracted several research funding from Portuguese, European, and international grant agencies. He has published nearly 200 international peer-reviewed journal articles, conference papers, and books. He has attended eight Ph.D. defenses as an opponent in various international universities. His research interests include autonomous aerial vehicles (AAV) communications, the age of information, cooperative relay communications, underwater wireless, RF energy harvesting in wireless networks, LDPC codes, 5G communications technologies, and NOMA. His teaching interests are in general communication engineering-related modules, such as the fundamentals of telecommunications, signal and systems, 5G wireless communications, cooperative communications at undergraduate, and master's and doctoral levels. He is a fellow of IET. He has received the Best Paper Award from IEEE ICCMIT, in 2017, and the International Conference on Emerging Technologies of Information and Communications, in March 2019, and the First Runner Up Best Paper Award from IRC 2023. In July 2019, he received the Education Leadership Award from the World Academic Congress, in 2019. In 2017 and 2018, he received the Outstanding Faculty Award from TPU. He also received the Distinguished Researcher in Wireless Communications Award in Chennai, India, in 2019. He was ranked as the Top 2% Scientist in the world by Stanford Elsevier list, in 2020, 2021, 2022, and 2023. He received the presidential award for outstanding research performance, in 2021. In 2021, he received the presidential award for his outstanding research performance among many other awards and recognitions. He is active in organizing conferences and workshops in the wireless communications area. He served as the TPC Chair for IEEE CIoT 2023, Lisbon, Portugal, the General Chair for IEEE ICIAfS 2021, Colombo, and the General Chair for the first IRC Sri Lanka, in 2022.